

***k*-resolved inverse photoemission of four different 6H-SiC (0001) surfaces**

C. Benesch, M. Fartmann, and H. Merz

Physikalisches Institut der Universität Münster, D-48149 Münster, Germany

(Received 12 June 2001; published 6 November 2001)

We have investigated the unoccupied electronic states of the Si-terminated (0001) surface of hexagonal 6H-SiC. The main problem with these surfaces is the reliable preparation of well defined surface reconstructions. We give reproducible methods to prepare the (1×1) , $(\sqrt{3} \times \sqrt{3})R30^\circ$, (3×3) , and the $(6\sqrt{3} \times 6\sqrt{3})R30^\circ$ surface by controlled heating of the SiC sample in a Si flux. These surface reconstructions show a characteristic LEED pattern and a characteristic Si/C peak ratio in Auger electron spectroscopy. We present *k*-resolved inverse photoemission spectra for the (1×1) , $(\sqrt{3} \times \sqrt{3})R30^\circ$, and (3×3) surface. We compare the measured dispersion relations with *ab initio* local density approximation surface band structure calculations of the (1×1) - and the $(\sqrt{3} \times \sqrt{3})R30^\circ$ -reconstructed 6H-SiC(0001) surface and with a Mott-Hubbard model of the electronic ground state of the $(\sqrt{3} \times \sqrt{3})R30^\circ$ and (3×3) reconstruction. The comparison between experiment and theory supports the Hubbard model: The experiment determines a value of $U=2.0$ eV for the Mott-Hubbard Coulomb interaction parameter for the $(\sqrt{3} \times \sqrt{3})R30^\circ$ reconstruction and $U=1.25$ eV for the (3×3) -reconstructed surface, respectively.

DOI: 10.1103/PhysRevB.64.205314

PACS number(s): 73.20.At

I. INTRODUCTION

Siliconcarbide (SiC) has become an interesting material for short wavelength optoelectronic, high temperature, radiation resistant, and high-power/high-frequency electronic devices because of its wide energy bandgap, its high thermal conductivity, its high breakdown electric field and its high saturated electron drift velocity.

For the realization and optimization of the technological application of SiC in the field of electronic devices, the reliable knowledge of the electronic structure of this semiconductor is advantageous. It is not only the electronic structure of the bulk, but also of the different free surfaces, which is of high interest.

In this work we investigate the electronic surface band structure of all four known 6H-SiC(0001) surface reconstructions with inverse photoemission (IPE). Therefore we need well prepared and characterized surfaces and we give reproducible methods for preparing the four surface reconstructions. The quality of the preparation is controlled by low-energy electron diffraction (LEED) and Auger electron spectroscopy (AES). At well prepared surfaces angle-resolved inverse photoemission spectra were performed and with these spectra several surface states of the different reconstructions of the 6H-SiC(0001) surface were determined.

II. EXPERIMENTAL

The inverse photoemission spectra were performed in an UHV chamber, additionally equipped with a LEED optic and a cylindrical mirror analyzer (CMA) for Auger electron spectroscopy. During the measurement the base pressure was about $1-2 \times 10^{-10}$ mbar.

The IPE setup is built by a band-pass Geiger-Müller counting tube and a modified version of the Erdman-Zipf electron gun¹ and it works in the isochromat mode with a fixed photon energy of 9.9 eV. The Geiger-Müller counting tube uses the combination of a CaF₂ entrance window with

an acetone filling. The ionization threshold of the gas and the transmission cutoff of the window define the energy band-pass of the detector.² With this combination an overall resolution in the IPE spectra (detector and electron gun) of ± 0.2 eV is achieved (determined by the 10–90 % onset at the Fermi edge in the IPE spectrum of polycrystalline tantalum).

The electron gun is a modified version of the Erdman-Zipf electron gun with a barium-oxide dispenser cathode. The gun supplies an electron beam with kinetic energies between 0 and 30 eV with the above mentioned resolution of ± 0.2 eV and a maximum sample current of a few μ A. The angle divergence is determined by Schäfer to $0.8-1.0$ nm⁻¹.³

The azimuthal incidence angle (or the direction of k_{\parallel} within the Brillouin zone) is adjusted using the LEED pattern. The polar angle is calibrated with a laser beam reflected by the surface of the sample: For the calibration procedure the electron gun is removed and replaced by a laser. If the laser beam and its reflected beam coincide, the sample is positioned in the normal incidence position (0°).

For temperature measurements of the sample an infrared pyrometer (emission factor of 6H-SiC: $\alpha = 85\%$) is used. The sample is heated by electron bombarding the back of the sample holder.

The Si-terminated, *p*-doped (A1) 6H-SiC wafer ($N_A = 6.2 \times 10^{17}$ cm⁻³, orientation on axis) was introduced into the UHV chamber as delivered by Cree Inc.⁴ without any previous chemical cleaning or etching. The four different surfaces (1×1) , $(\sqrt{3} \times \sqrt{3})R30^\circ$, (3×3) , and $(6\sqrt{3} \times 6\sqrt{3})R30^\circ$ were prepared by heating the sample in a Si flux. The Si flux was produced by an UHV evaporator with an integral flux monitor from Omicron (EFM). The flux monitor continuously monitors the evaporation rate by measuring the ion current (in nA), which is proportional to the flux of neutral Si atoms. This allows a reproducible flux adjustment and a fast flux control.

The position of the Fermi edge of the apparatus is calibrated by taking a reference IPE spectrum of polycrystalline tantalum (which is mounted on a second sample holder). The

TABLE I. Summary of the preparation parameters for the four different 6H-SiC(0001) surfaces.

Surface		Si flux Φ [nA]	time t [min]	temp. T [°C]
(1×1)	1. step	≥ 40	10	800
	2. step		10–20	930
$(\sqrt{3} \times \sqrt{3})R 30^\circ$		15–20	10	930
(3×3)		40	10	860
$(6\sqrt{3} \times 6\sqrt{3})R 30^\circ$			10	980

steep onset in the tantalum IPE spectrum gives the position of the Fermi level E_F of the apparatus.

The equation

$$k_{\parallel}(E_i) = \hbar^{-1} \sqrt{2m(E_i - \Phi)} \sin \vartheta$$

is used for the calculation of the $E(k_{\parallel})$ dispersion. In this equation E_i is the energy of the incoming electrons (with respect to the Fermi level of the sample), ϑ is the angle between the electron beam and the sample normal, and Φ is the work function of the sample. The work function is measured by a combined evaluation of target current spectroscopy (TCS) and IPE: The onset in the target current gives the difference between the work function of the sample and the work function of the cathode. The work function of the cathode is separately measured by the onset within an IPE spectrum of polycrystalline tantalum. With these combined techniques we determine the work function of the 6H-SiC(0001) surface to $\Phi = (4.8 \pm 0.2)$ eV, in good agreement with Pelletier *et al.*⁵ $\Phi = (4.85 \pm 0.10)$ eV.

A. Sample preparation

In this work the (1×1) , $(\sqrt{3} \times \sqrt{3})R 30^\circ$, (3×3) , and $(6\sqrt{3} \times 6\sqrt{3})R 30^\circ$ reconstructions of the 6H-SiC(0001) surface were prepared by heating the sample in a controlled Si flux. With this method well-ordered reconstructions were produced, which not only show good LEED pattern, but also—which is more demanding—well structured reproducible inverse photoemission spectra. The different reconstructions were characterized by LEED and—independently—by Auger electron spectroscopy (AES). The different reconstructions have different characteristic AES-Si/C peak ratios (see Table II). Dependent on the offered silicon flux and the heating temperature of the sample a well defined narrow interval for the Si/C peak ratio for each reconstruction was found. Thus for the preparation of a definite surface reconstruction the three parameters (i) time of preparation, (ii) silicon flux, and (iii) heating temperature of the sample have to be chosen within narrow intervals. Table I shows the used preparation parameters for all prepared reconstructions.

1. (1×1) surface

The (1×1) surface was prepared in two steps: Starting from a surface with a low Si/C ratio the sample was annealed in a first step at a temperature of $T = 800^\circ\text{C}$ in a Si flux of 40 nA for 10 min. With this preparation the amount of silicon at

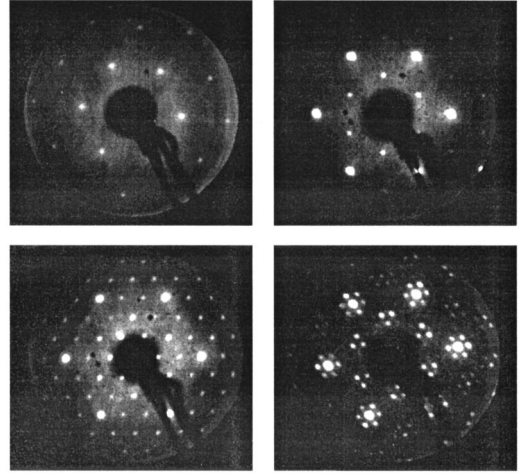


FIG. 1. LEED pattern of the four discussed 6H-SiC(0001) surfaces: (1×1) at 180 eV, $(\sqrt{3} \times \sqrt{3})R 30^\circ$ at 99 eV, (3×3) at 98 eV, and $(6\sqrt{3} \times 6\sqrt{3})R 30^\circ$ at 105 eV.

the surface increases. If the AES-Si/C-peak ratio reaches values ≥ 6 the Si flux was stopped and the next preparation step was started. The sample was annealed for 10 min at a higher temperature of $T = 930^\circ\text{C}$. Without an offered Si flux this heating procedure reduces the amount of silicon at the surface and at this temperature the surface shows a (1×1) -LEED pattern as seen in Fig. 1. The sharpness of the LEED spots shows that these two steps are a suitable preparation method for the (1×1) surface. The surfaces prepared in this way show no oxygen peak in the AES spectra and an AES-Si/C peak ratio of about 1 in good agreement with van Elsbergen *et al.* (1.0 ± 0.5) ⁶ and Kaplan (< 2).⁷ The AES-Si/C peak ratio of the (1×1) surface is the lowest Si/C ratio of the four surfaces investigated in this paper.

2. $(\sqrt{3} \times \sqrt{3})R 30^\circ$ reconstruction

The $(\sqrt{3} \times \sqrt{3})R 30^\circ$ reconstruction can be prepared by annealing the sample at a temperature of $T = 930^\circ\text{C}$ in a silicon flux of 15–20 nA for 10 min. The optimal value of the Si flux depends on the previous state of preparation: If the preparation procedure starts at an AES-Si/C peak ratio of about 6 [e.g., with a preceding (3×3) -reconstructed surface] a Si flux of 15 nA or even less is required, but when starting with an AES-Si/C peak ratio of 1 [e.g., from the (1×1) surface] a higher Si flux of 20 nA is needed. Figure 1 shows the LEED pattern of the $(\sqrt{3} \times \sqrt{3})R 30^\circ$ reconstruction. This surface exhibits an AES-Si/C peak ratio between 4 and 5, in good agreement with van Elsbergen *et al.* (4.3 ± 2.2) ⁶ and Kaplan (3.2 ± 0.4) .⁷ The value of 4–5 shows that the $(\sqrt{3} \times \sqrt{3})R 30^\circ$ reconstruction is a silicon rich surface. The $(\sqrt{3} \times \sqrt{3})R 30^\circ$ reconstruction shows no change in the AES spectra or the LEED pattern for hours but it is not very stable concerning taking good IPE spectra (see Sec. II B). After a first successful preparation the $(\sqrt{3} \times \sqrt{3})R 30^\circ$ reconstruction can be reprepared easily and quickly by heating the sample at the above mentioned temperature of $T = 930^\circ\text{C}$ for 5 min with no or only a small Si flux. Repeating this procedure in regular intervals is necessary for taking well structured IPE spectra (see Sec. II B).

TABLE II. Summary of the AES-Si(*L*VV)/C(*K*VV) peak intensity ratios of the different 6H-SiC(0001) surfaces.

Surface	AES-Si(<i>L</i> VV)/C(<i>K</i> VV)-peak ratio		
	This work	v. Elsbergen <i>et al.</i> ^a	Kaplan ^b
(3×3)	6–7	7.8±2.1	5.5±0.4
(√3×√3) <i>R</i> 30°	4–5	4.3±2.2	3.2±0.4
(6√3×6√3) <i>R</i> 30°	1.0–1.7	<2.2	
(1×1)	≈1	1.0±0.5	<2

^aFrom Ref. 6.

^bFrom Ref. 7.

3. (3×3) reconstruction

To prepare the (3×3) reconstruction a relatively low preparation temperature of $T=860^\circ\text{C}$ and a relatively high silicon flux (40 nA) is required for about 10 min. With these conditions the amount of silicon at the surface rises; well prepared (3×3) surfaces (e.g., see Fig. 1) show an AES-Si/C ratio of 6 to 7, again in agreement with van Elsbergen *et al.* (7.8±2.1)⁶ and Kaplan (5.5±0.4)⁷. The (3×3) reconstruction is the silicon richest surface of 6H-SiC discussed in this paper.

4. (6√3×6√3)*R*30° reconstruction

Starting from a (√3×√3)*R*30° reconstruction a (6√3×6√3)*R*30° reconstruction is prepared by annealing the sample at a temperature of $T=980^\circ\text{C}$ for 10 min without any additional silicon flux as reported by van Elsbergen *et al.*⁶ If one starts from a (3×3) reconstruction with a high AES-Si/C ratio the time of preparation is somewhat longer. In any case the (6√3×6√3)*R*30° reconstruction is reached, identified by the LEED pattern shown in Fig. 1. AES shows that this reconstruction is a surface with a low amount of Si. An AES-Si/C peak ratio of 1.7 was measured in good agreement with van Elsbergen *et al.* (<2.2).⁶

5. Summary of the preparation parameters

The good quality of the LEED patterns (Fig. 1) and the IPE spectra (see Sec. II B) show that suitable preparation conditions for the four different 6H-SiC(0001) surfaces were found. The preparation parameters are summarized in Table I. Surfaces prepared in this way show characteristic AES-Si/C peak ratios. In Table II a summary of the Auger electron intensity ratios $\text{Si}_{L_{VV}}/\text{C}_{K_{VV}}$ is given. The comparison with the values of van Elsbergen *et al.*⁶ and Kaplan⁷ shows that the AES-Si/C peak ratios agree within narrow intervals: The Si/C ratio decreases from the (3×3) reconstruction over the (√3×√3)*R*30° and the (6√3×6√3)*R*30° reconstruction to the (1×1) surface.

B. IPE

At the 6H-SiC(0001) surface reconstructions, prepared in the above mentioned way, inverse photoemission spectra can be taken successfully. Thereby the electron energy is scanned between -2.0 and 12.0 eV (with respect to the Fermi level of the sample) in steps of 0.1 eV. Because the Fermi level of

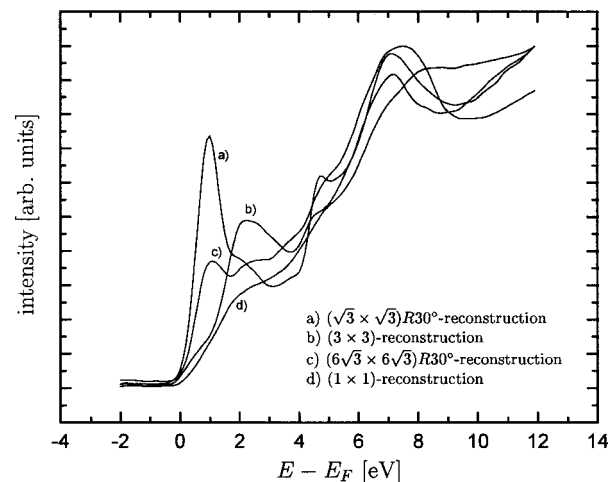


FIG. 2. Comparison of the normalized normal incidence inverse photoemission spectra of the four discussed 6H-SiC(0001) surfaces.

a semiconductor such as SiC is within the bulk bandgap, the Fermi energy is separately determined by a reference IPE spectrum taken at tantalum. If the tantalum sample and the SiC sample have an ohmic contact, the position of the Fermi level of the SiC wafer can be determined by measuring the onset in the IPE spectrum of the metallic tantalum sample. The exact position of the Fermi level is determined by the maximum of the first derivation at this onset.

Typical measuring times of the IPE spectra were 9.9 s per point or in total 23.5 min per run. The sample current was a few μA at all measurements and the maximum counting rate was about 15 000 counts per 9.9 s with an background of 3 to 4 counts per 9.9 s. For the subsequent evaluation of the structures in the IPE spectra up to 10 runs were summarized and a total measuring time per point of up to 99 s was achieved. The maximum of counts was about 150 000. For the angle-resolved investigations such spectra are needed for each angle position.

III. RESULTS AND DISCUSSION

Figure 2 shows normalized normal incidence IPE spectra of the four different 6H-SiC(0001) surfaces. The IPE spectra of the different reconstructions differ considerably, thus an identification of a given reconstruction is also possible by IPE.

Each spectrum shows significant structures which are discussed in the following section. The exact energetic position of the peaks is determined by taking the minima of the second derivation of the spectra. After many repeated preparations of the same surface reconstruction this procedure gives the position of the peaks within an uncertainty of ± 0.1 eV.

A. (1×1) surface

Figure 3 shows angle-resolved IPE spectra of the (1×1) surface in $\overline{\Gamma K}$ and $\overline{\Gamma M}$ directions. Four different structures at (1.8±0.1) eV, (4.7±0.1) eV, (6.9±0.1) eV, and (8.0±0.1) eV can be determined for the normal incidence (0°) spectrum.

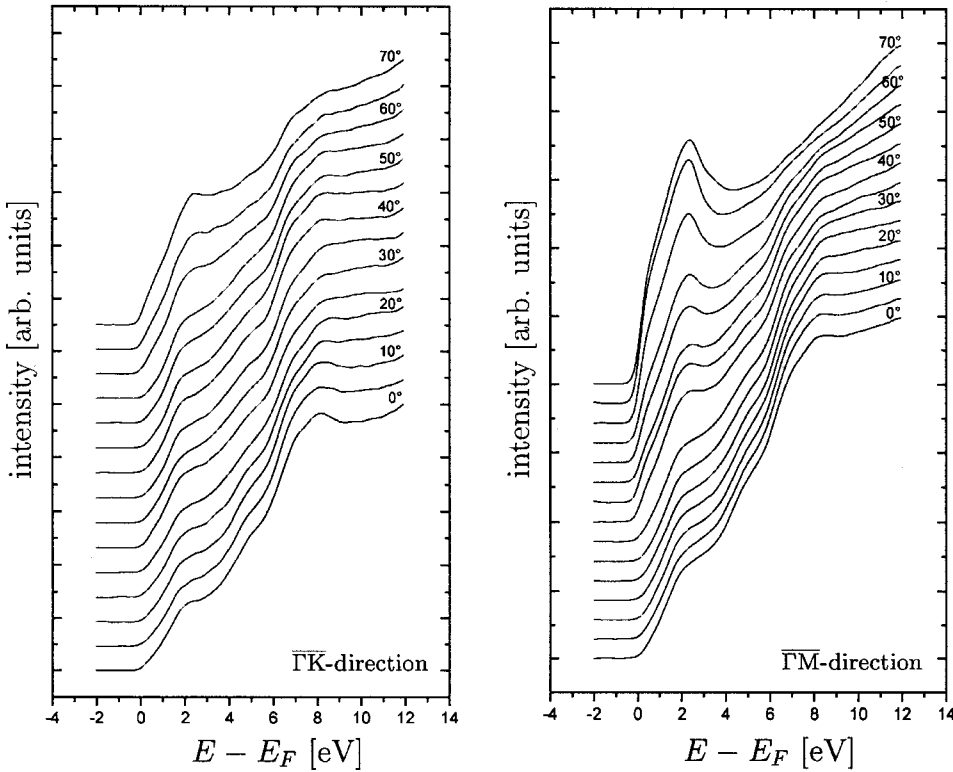


FIG. 3. Angle-resolved inverse photoemission spectra of the (1×1) surface of 6H-SiC in the high symmetry directions $\overline{\Gamma K}$ and $\overline{\Gamma M}$ of the first Brillouin zone.

An inverse photoemission spectrum at an incidence of 0° taken after seven days without a fresh preparation shows no significant difference: Both spectra have the same shape and the peaks are at the same position. That means the (1×1) surface is a relatively stable surface concerning taking inverse photoemission spectra. This statement is confirmed by LEED and AES measurements after these seven days: The LEED pattern is found as sharp and with the same intensity as at the freshly prepared surface, and in the AES spectra there is no difference in the Si/C ratio. After an exposure of 30, 180, 500, and 3300 L oxygen we found no difference between the IPE spectra, the LEED pattern or the AES-Si/C peak ratio and there is only a very weak oxygen peak in the AES spectrum. This means that the (1×1) surface represents a low reactivity surface. The fresh prepared (1×1) surface is not oxide covered, because at well prepared surfaces there is no oxygen signal in the AES spectra. Probably the surface is saturated with hydrogen, which is not detectable with AES. This coverage could explain the low reactivity of this surface.

For the angle-resolved IPE spectra (Fig. 3) the angle between the normal of the sample and the electron beam is increased from 0° to 70° in steps of 5° in both of the high symmetry directions $\overline{\Gamma K}$ and $\overline{\Gamma M}$. The spectra in the $\overline{\Gamma K}$ direction are relatively similar to each other and they all show the above mentioned four peaks observed in normal incidence. The intensity of the peak at 4.9 eV decreases with higher angles and at 70° it almost has disappeared. The spectra in $\overline{\Gamma M}$ direction are more different to each other. The four peaks can clearly be distinguished in this direction, too. The intensity of the peak at 8.0 eV decreases and the intensity of the peak at 1.8 eV increases with growing polar angle. At an

angle of 35° an additional peak at an energy of (0.3 ± 0.1) eV becomes visible, its intensity increases to larger angles. This feature around the \overline{M} point is a Fermi step, thus the experiment shows that the (1×1) surface is a metallic surface.

From these angle-resolved IPE spectra we plot the $E(k_{\parallel})$ dispersion diagrams. Figure 4 shows the dispersion relation $E(k_{\parallel})$ in $\overline{\Gamma K}$ and $\overline{\Gamma M}$ directions of the (1×1) surface. All four bands show only a weak dispersion up to 0.5 eV.

For a comparison between experimental data and theoretical surface band structure calculations the exact energetic position of the Fermi level with respect to valence band maximum (VBM) for the examined p -doped 6H-SiC sample is needed. The position of the bulk Fermi level has been determined by Pelletier *et al.* for p -doped 6H-SiC ($N_A = 10^{24} \text{ m}^{-3}$) at room temperature to $E_F - E_{\text{VBM}} = 0.18 \text{ eV}$,⁵ but to the best of our knowledge there is no determination of the energetic position of the Fermi level with respect to VBM of one of the surfaces discussed in this paper for a p -doped 6H-SiC sample. Because there is no possibility to determine the absolute position of the Fermi level with respect to VBM in our apparatus so far, it is not possible to compare the absolute energetic position of the experimentally measured peaks with theoretically calculated LDA band structures of the same surface.

Theoretical surface band structure calculations using local density approximation (LDA) by Sabisch *et al.*⁸ show a half filled surface band at an energetic position of 2.1 eV above VBM and a completely unoccupied surface band 5.5 eV above VBM at the $\overline{\Gamma}$ point. The surface state at an energetic position of 2.1 eV (D_{Si}) might be correlated to the measured

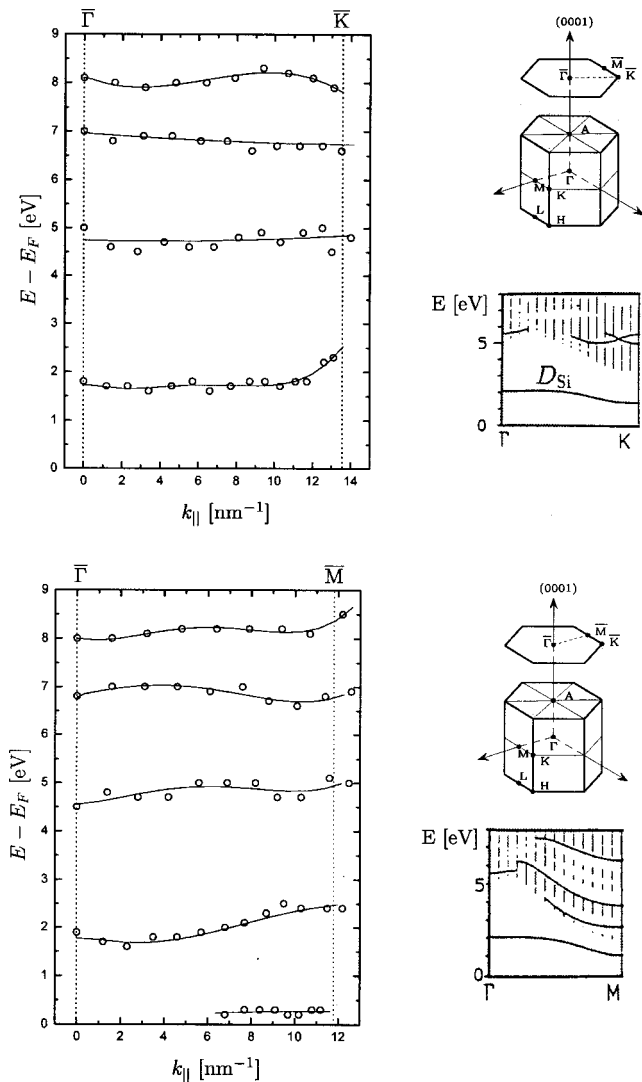


FIG. 4. Experimental dispersion relations of the (1×1) surface of 6H-SiC(0001) in the $\Gamma\bar{K}$ (upper part) and $\Gamma\bar{M}$ directions (lower part) together with a LDA calculation of the surface band structure of Sabisch *et al.* (Ref. 8).

1.8 eV peak because both structures are the lowest structures of this surface with unoccupied electronic states. Thus the origin of the experimentally determined peak at 1.8 eV could be identified as a surface state. If the measured and the theoretically calculated structure correspond to each other, the energetic position of the Fermi level of the (1×1) surface can be estimated as the difference between the energetic position of the surface peak in LDA calculation (2.1 eV) with respect to VBM and the energetic position of the experimentally determined peak position (1.8 eV) with respect to the Fermi level of the (1×1) surface. The resulting value of 0.3 eV for the energetic position of the Fermi level with respect to VBM is in the region of the bulk Fermi level [$E_F - E_{VBM} = 0.18$ eV (Ref. 5)]. The experiment shows no dispersion in the $\Gamma\bar{K}$ direction and an upward dispersion of 0.5 eV in the $\Gamma\bar{M}$ direction. This is in contrast to LDA calculations which clearly shows a downward dispersion of about 1 eV in both of the high symmetry directions. The measured

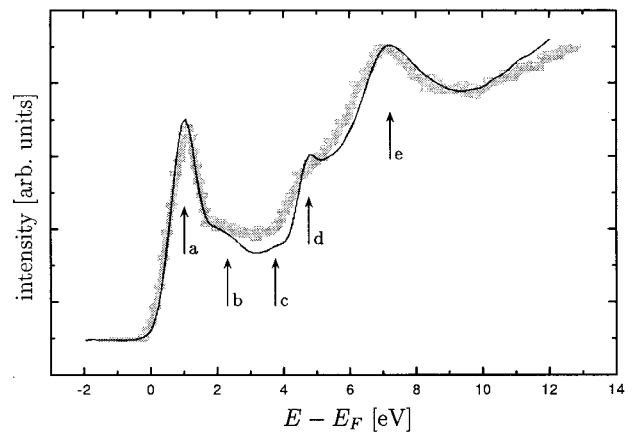


FIG. 5. Normal incidence inverse photoemission spectrum of the $(\sqrt{3} \times \sqrt{3})R30^\circ$ -reconstructed 6H-SiC(0001) surface (solid curve) in comparison with an IPE spectrum taken by Themlin *et al.* (Ref. 9) (shaded).

peak at 4.7 eV is not corresponding to a surface structure within the theoretical calculations. Because there is no experimental determined structure near the theoretical 5.5 eV peak this surface band could correspond to the experimentally determined structure, although the calculated dispersion in $\Gamma\bar{M}$ direction is much larger than the experimentally determined. The energetic positions of the third and fourth measured peak at 6.9 and 8.0 eV are in an area without any calculated surface states but only (projected) bulk states. The LDA calculations for the (1×1) surface and the experiment do not agree very well.

B. $(\sqrt{3} \times \sqrt{3})R30^\circ$ reconstruction

Figure 5 shows an IPE spectrum performed at the $(\sqrt{3} \times \sqrt{3})R30^\circ$ -reconstructed surface under normal incidence taken by the authors (full curve) and by Themlin *et al.*⁹ (shaded curve). The spectrum shows five main structures: A well developed peak at (1.0 ± 0.1) eV [peak (a)], two peaks with lower intensity at (2.2 ± 0.1) eV and at (3.5 ± 0.1) eV [peaks (b) and (c)], a well developed one at (4.6 ± 0.1) eV [peak (d)] and at (7.1 ± 0.2) eV [peak (e)]. The 2.2 eV and the 3.5 eV peak can only be separately resolved with the ± 0.2 eV resolution of the used Geiger-Müller counting tube (see Fig. 5).

The $(\sqrt{3} \times \sqrt{3})R30^\circ$ reconstruction is much less stable concerning taking IPE spectra than the (1×1) reconstruction. Figure 6 shows a series of IPE spectra taken at the $(\sqrt{3} \times \sqrt{3})R30^\circ$ reconstruction under normal incidence. Within a few hours the intensity of the lower-energy peaks and especially of the first one decreases significantly. This decrease of intensity is caused by the contamination of the surface by residual gas within the UHV chamber. Although all IPE spectra were taken at a base pressure of about $1 - 2 \times 10^{-10}$ mbar the intensity of the peak at 1.0 eV [peak (a)], the peak at 2.2 eV [peak (b)] and the 4.6 eV peak [peak (d)] decreases. This is an experimental indication that the origins of these peaks are surface states. The decrease in intensity makes it necessary to reprepare these surface reconstruction after each taken IPE run.

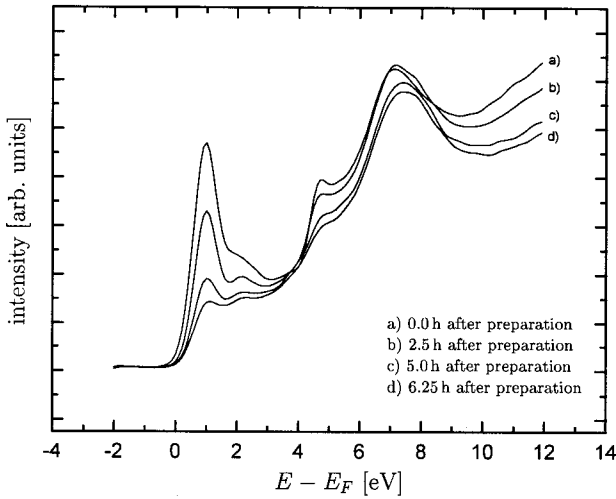


FIG. 6. Time evolution of the normal incidence inverse photoemission spectrum of the $(\sqrt{3}\times\sqrt{3})R30^\circ$ -reconstructed 6H-SiC(0001) surface.

Figure 7 shows angle-resolved IPE spectra taken at the $(\sqrt{3}\times\sqrt{3})R30^\circ$ -reconstructed 6H-SiC(0001) surface in the $\overline{\Gamma K}$ and $\overline{\Gamma M}$ directions. All spectra show the abovementioned five peaks (a)–(e). The different intensities of peak (a) are caused by the fact, that the time interval between the end of the preparation and start of the next IPE run varied within a few minutes, thus the intensities of peak (a) cannot be compared exactly with each other. But the peak positions are not related to the intensity and that makes it possible to produce $E(k_{\parallel})$ diagrams from these spectra.

Figure 8 shows the dispersion relation $E(k_{\parallel})$ in the $\overline{\Gamma K}$ and $\overline{\Gamma M}$ directions. The structure at an energetic position of 1.0 eV [peak (a)] shows a slight downward dispersion of 0.1 eV in the $\overline{\Gamma M}$ and $\overline{\Gamma K}$ directions. The second band at 2.2 eV [peak (b)] shows a downward dispersion to 2.0 eV in the $\overline{\Gamma K}$ direction in the middle of the $\overline{\Gamma}$ and \overline{K} points and then an upward dispersion up to 2.8 eV and ends at 2.5 eV at the \overline{K}

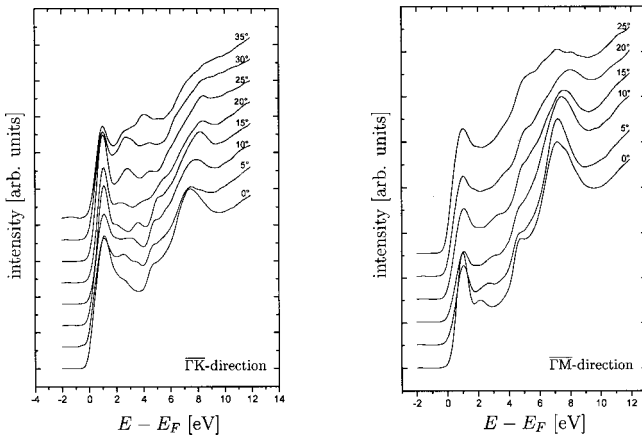


FIG. 7. Angle-resolved inverse photoemission spectra of the $(\sqrt{3}\times\sqrt{3})R30^\circ$ -reconstructed 6H-SiC(0001) surface in the high symmetry directions $\overline{\Gamma K}$ and $\overline{\Gamma M}$.

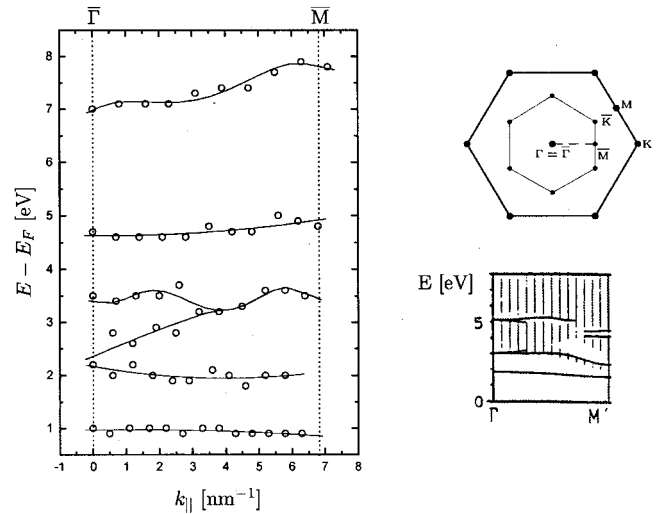
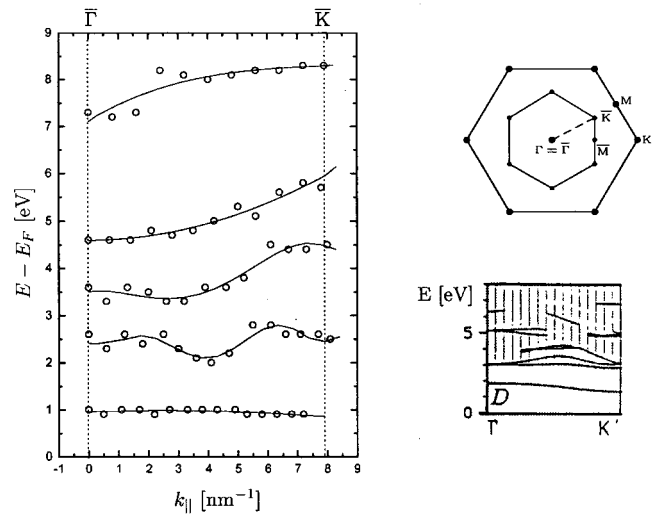


FIG. 8. Experimental dispersion relations of the $(\sqrt{3}\times\sqrt{3})R30^\circ$ -reconstructed 6H-SiC(0001) surface in the $\overline{\Gamma K}$ (upper part) and $\overline{\Gamma M}$ directions (lower part) together with a LDA calculation of the surface band structure of Sabisch *et al.* (Ref. 8).

point. In the $\overline{\Gamma M}$ direction the band is splitting. One branch has a slight downward dispersion from 2.2 eV at the $\overline{\Gamma}$ point to 2.0 eV around the \overline{M} point and the other band has an upward dispersion from 2.2 eV at the $\overline{\Gamma}$ point to 3.2 eV in the middle of the $\overline{\Gamma M}$ direction. Here it joins the next band [peak (c)]. This band with an energetic position of 3.5 eV at the $\overline{\Gamma}$ point has a wavelike dispersion in the $\overline{\Gamma M}$ direction. In the $\overline{\Gamma K}$ direction the structure at 3.5 eV has a flat dispersion to the middle of the $\overline{\Gamma K}$ direction and then an upward dispersion up to 4.5 eV. The dispersion of the two peaks (b) and (c) is difficult to determine, because of the small peak heights in the IPE spectra. The determination of the dispersion of peak (a) and the next two peaks (d) and (e) is easier. Band (d) at 4.6 eV at the $\overline{\Gamma}$ point has a small upward dispersion of 0.4 eV in the $\overline{\Gamma M}$ direction and a larger dispersion of 1.2 eV in the $\overline{\Gamma K}$ direction. The band at an energetic position of 7.1 eV

at the $\bar{\Gamma}$ point shows an upward dispersion of 1.1 eV in the first half of the $\bar{\Gamma}\bar{K}$ direction and an upward dispersion of 0.7 eV in the second half of the $\bar{\Gamma}\bar{M}$ direction.

Ab initio LDA calculations of Sabisch *et al.* show a half filled surface band (D) 1.8 eV above VBM.⁸ The dispersion of the surface state is slightly downwards to the \bar{K} and \bar{M} points, respectively, similar to the lowest experimental determined empty surface state, but in contrast to the theoretical calculation the IPE experiment shows only fully unoccupied surface states. Northrup *et al.* also found in LDA calculations a half filled surface state (Σ_1) at an energetic position of 1.3 eV above VBM at the $\bar{\Gamma}$ point dispersing downwards to 0.9 eV in the $\bar{\Gamma}\bar{K}$ direction and 1.3 eV in the $\bar{\Gamma}\bar{M}$ direction.¹⁰ Both calculations show a larger dispersion than the experiment and a metallic surface in contrast to the measured semiconducting surface. The first fully unoccupied calculated surface band at 3.0 eV above VBM, i.e., 1.2 eV above the half filled surface state at the $\bar{\Gamma}$ point, could correlate to the second experimentally determined surface structure, which energetic position is also 1.2 eV above the lowest unoccupied surface state. But the theoretical calculated and experimental determined dispersion is different (see Fig. 8). One reason for that difference could be the difficulty in determining the exact energetic position of the measured peaks in that area and the splitting of the surface bands in the theoretical calculations as well as in the experiment. The next calculated surface band 5.1 eV above VBM at the $\bar{\Gamma}$ point, i.e., 2.0 eV above the second surface state could correlate with the experimental determined structure 2.4 eV above the second experimentally determined band 4.6 eV above Fermi level. Again the dispersion is different (see Fig. 8) and the theoretical calculation has some breaks in the surface band, while the experiment shows a well established peak in all spectra. The measured 7.1 eV band (e) does not correspond to a theoretical surface band.

The comparison between LDA calculations and IPE spectra shows only a few agreements, and there are two contradiction to this point of view: First, both LDA calculations predict a half filled surface band, but the IPE experiment shows a fully unoccupied surface band. No half filled surface band has been detected experimentally. And second, in the presented IPE spectra and in those of Themlin *et al.*⁹ the position of the Fermi level is at the same energetic position (see Fig. 5), but our sample is p doped and the one from Themlin *et al.* is n doped. If the Fermi level of the surface is at the same energetic position as the Fermi level of the bulk, the position of the Fermi level of the n -doped sample should be in the upper part of the bandgap [$E_F - E_{\text{VBM}} > (1/2)E_{\text{gap}}$] and the position of the Fermi level of the p -doped sample should be in the lower part of the bandgap [$E_F - E_{\text{VBM}} < (1/2)E_{\text{gap}}$]. To explain these facts, a theory is needed in which the Fermi energy of the surface is the same for different doping types (band bending at the surface) and the theory should predict a semiconducting surface, i.e., fully occupied and fully unoccupied surface states.

Because of the narrow bandwidth of the abovementioned surface state (D or Σ_1) correlation effects can occur, which

are not taken into account by the cited one-electron-theory (LDA calculations). Based on a Hubbard model, in which the correlation energy U of the Si dangling bond is included, Northrup *et al.*, Rohlffing *et al.*, Furtmüller *et al.*, and Anisimov *et al.* have calculated a surface band structure for the $(\sqrt{3}\times\sqrt{3})R30^\circ$ reconstruction.^{11–14} They show, that the Mott-Hubbard model can explain the fully occupied and fully unoccupied surface states as the lower and upper Hubbard band and the position of the Fermi level of the surface, which is pinned between the lower and the upper Hubbard band, is independent of the bulk doping level. The presented IPE spectra taken at a p -doped SiC sample together with the IPE spectra of Themlin *et al.* taken at a n -doped sample support a strong band bending and a Fermi level pinning, because of the same energetic position of the Fermi level at samples of different doping types. Based on the Mott-Hubbard model Furtmüller *et al.* determine the Fermi level to be pinned 2.15 eV above VBM,¹³ which means the measured empty state 1.0 eV above E_F is placed 3.15 eV above VBM at the center of the SBZ. The measured dispersion of that peak in the $\bar{\Gamma}\bar{M}$ and $\bar{\Gamma}\bar{K}$ directions is weak and the corresponding surface band decreases slightly towards the \bar{K} and \bar{M} points. This course is parallel to the completely occupied photoemission structure measured by Mårtensson *et al.*¹⁵ as predicted by theory. At the center of the SBZ the direct photoemission experiment gives the energetic position of the occupied surface state to 1.1 eV above VBM. With this value the correlation parameter U can be estimate as the energy difference between the lower and the upper Hubbard band, i.e., the energy difference between the identified surface bands in PE and IPE spectra to $U=2.05$ eV. This value is in good agreement with the calculated $U\approx 2.1$ eV of Furtmüller *et al.* and $U=1.95$ eV of Rohlffing *et al.* and somewhat larger than the $U=1.5$ eV of Anisimov *et al.* and the $U=1.6$ eV of Northrup *et al.* The latter mentioned that additional electrons or holes introduced by doping could couple strongly to the adatom positional coordinates and this could lead to additional states near the Fermi level for doped surfaces. The similarity of our IPE spectra at p -doped SiC and the IPE spectra of Themlin *et al.* at n -doped samples shows, that there are no additional unoccupied states for p - or n -doped bulk material. The electronic structure of the $(\sqrt{3}\times\sqrt{3})R30^\circ$ reconstruction is independent of the doping type of the bulk.

In conclusion for the $(\sqrt{3}\times\sqrt{3})R30^\circ$ reconstruction, the presented IPE spectra show a few agreements with the one electron theory (LDA calculations), but because of the same Fermi level of the p - and n -doped $(\sqrt{3}\times\sqrt{3})R30^\circ$ -reconstructed SiC surface and the measured semiconducting surface, the presented study supports the Hubbard model with an experimental determined correlation parameter of $U=2.05$ eV.

C. (3×3) reconstruction

Figure 9 shows an IPE spectrum (solid line) in comparison to an IPE spectrum taken by Themlin *et al.*⁹ (shadowed). These spectra agree well. Six different peaks can be distinguished within these spectra at (0.6 ± 0.1) eV [peak (a)], at

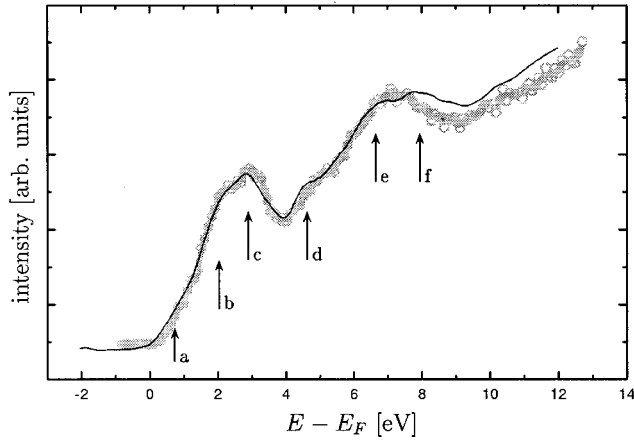


FIG. 9. Normal incidence inverse photoemission spectrum of the (3×3) reconstruction (solid curve) in comparison with an IPE spectrum measured by Themlin *et al.* (Ref. 9) (shaded).

(1.8 ± 0.1) eV [peak (b)], at (2.8 ± 0.1) eV [peak (c)], at (4.6 ± 0.1) eV [peak (d)], at (6.5 ± 0.1) eV [peak (e)], and at (8.1 ± 0.1) eV [peak (f)] with respect to the Fermi level of the sample.

The (3×3) reconstruction is not as stable concerning taking inverse photoemission spectra as the (1×1) reconstruction (stable for a few days) but more stable than the $(\sqrt{3} \times \sqrt{3})R30^\circ$ reconstruction (stable for only one spectrum). After a fresh preparation IPE spectra can be taken for a few hours (3 h – 5 h), i.e., some spectra at different angles can be performed without a new preparation.

Figure 10 shows angle-resolved IPE spectra of the (3×3) reconstruction in the $\overline{\Gamma KMK}$ and $\overline{\Gamma M}$ directions. Figure

11 shows the dispersion relation $E(k_{\parallel})$ in the $\overline{\Gamma KMK}$ and $\overline{\Gamma M}$ directions. In the $\overline{\Gamma M}$ direction all six peaks show no, or only a weak dispersion. In the $\overline{\Gamma K}$ direction the peak at 0.6 eV shows also only a weak dispersion of 0.1 eV downward to the \overline{K} point. Peak (b) shows a small upward dispersion in the first half of the $\overline{\Gamma K}$ direction and a small downward dispersion in the second part of the $\overline{\Gamma K}$ direction. In the \overline{KMK} direction peak (b) shows no dispersion. Peak (c) shows a small wavelike dispersion in the $\overline{\Gamma KMK}$ direction and peak (d) shows no dispersion in the $\overline{\Gamma K}$ direction and an upward dispersion of 0.5 eV in the \overline{KMK} direction. Peak (e) shows also no dispersion in the $\overline{\Gamma K}$ direction, in the \overline{KM} direction a downward, and in the \overline{MK} direction an upward dispersion. Peak (f) shows a downward dispersion of 0.8 eV to the \overline{K} point, in the \overline{KMK} direction the dispersion is upward to the \overline{M} point and downward to the \overline{K} point.

At this reconstruction again there is the fact, that the Fermi level of our *p*-doped sample and the Fermi level of the *n*-doped sample of Themlin *et al.*⁹ are very similar (see Fig. 9). This means, that there is a band bending at this surface, too, so that the Fermi levels of the different doped samples are nearly identical. Furthermore, the spectra show completely empty surface structures, thus the (3×3) reconstruction is a semiconducting surface.

As an analog to the $(\sqrt{3} \times \sqrt{3})R30^\circ$ -reconstructed surface, Furthmüller *et al.*¹³ suggested a Mott-Hubbard model for this surface with a Hubbard parameter of $U \approx 1$ eV to explain the semiconducting character of this surface, because in photoemission experiments they found a completely occupied surface state 1.3 eV above VBM but below the Fermi level

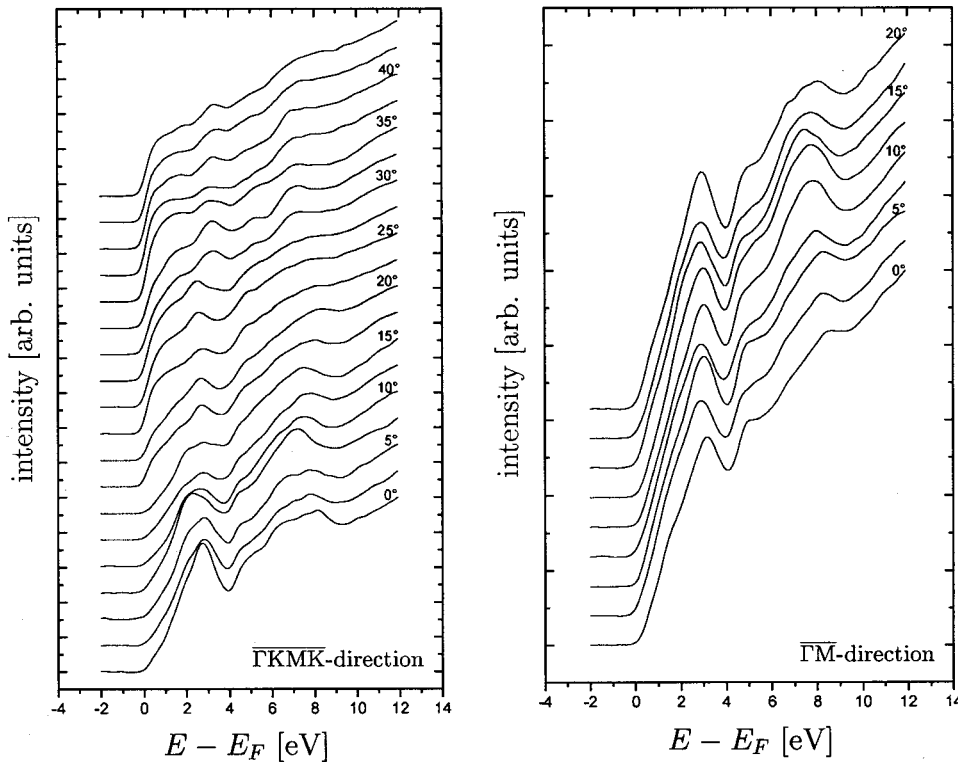


FIG. 10. Angle-resolved inverse photoemission spectra of the (3×3) -reconstructed $6H$ -SiC(0001) surface in high symmetry directions $\overline{\Gamma K}$ and $\overline{\Gamma M}$.

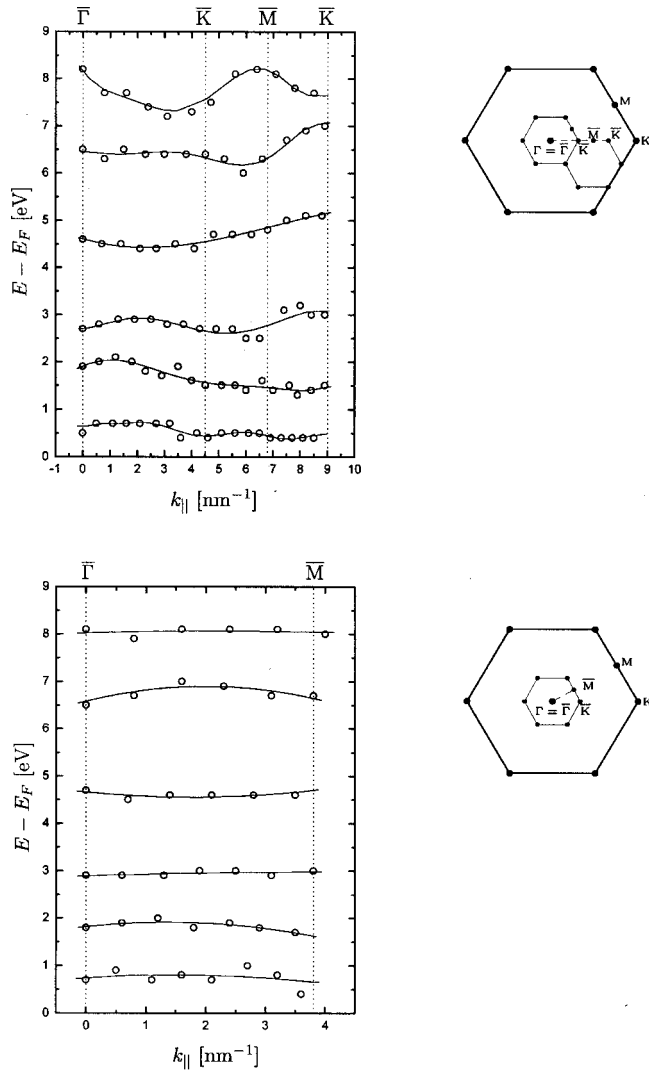


FIG. 11. Experimental dispersion relations of the (3×3) -reconstructed 6H-SiC(0001) surface in the $\Gamma\bar{K}$ (upper part) and $\Gamma\bar{M}$ directions (lower part).

(pinned 1.95 eV above VBM). This surface band shows no dispersion along the high symmetry directions.

With that position of the Fermi level the first measured peak at an energetic position of 0.6 eV with respect to E_F is 2.55 eV above VBM within the bulk bandgap. This position within the bulk bandgap is an indication for the surface character of this peak. It shows no dispersion in the $\Gamma\bar{M}$ and $\Gamma\bar{K}$ directions. This fully unoccupied surface state and the completely occupied surface state determined with direct photoemission can be identified as the lower and upper Hubbard band, and from the energetic difference of the highest occupied and lowest unoccupied surface state the correlation parameter U can be estimated to $U = 1.25$ eV. This value is in good agreement with the calculated value of ≈ 1 eV from Furthmüller *et al.* and also in agreement with Johansson *et al.*, who determined the surface bandgap by an angle-resolved direct and inverse photoemission to 1.0 eV (Ref. 16) also supporting the Mott-Hubbard model.

In summary for the (3×3) reconstruction we support the Mott-Hubbard model, because of the completely unoccupied

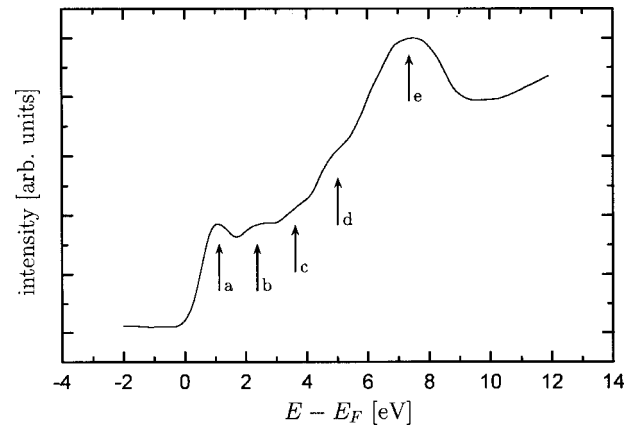


FIG. 12. Normal incidence IPE spectrum of the $(6\sqrt{3} \times 6\sqrt{3})R30^\circ$ -reconstructed 6H-SiC(0001) surface.

(IPE) and the completely occupied (PE) measured surface bands and the extremely similar IPE spectra of p - and n -doped samples with a nearly identical position of the surface Fermi level. That means the Fermi level of the surface is different from the Fermi level of the bulk, and there is a band bending which pins the Fermi levels of p - and n -doped SiC at the same energetic position. The Fermi level of the surface is independent of the doping type of the bulk material.

D. $(6\sqrt{3} \times 6\sqrt{3})R30^\circ$ reconstruction

Figure 12 shows an IPE spectrum at normal incidence of the $(6\sqrt{3} \times 6\sqrt{3})R30^\circ$ reconstruction. To the best of our knowledge there is no theoretical band structure calculation for this reconstruction. The first Brillouin zone at the surface of the $(6\sqrt{3} \times 6\sqrt{3})R30^\circ$ reconstruction is so small (1.1 nm^{-1} in the $\Gamma\bar{M}$ direction), that it is not meaningful to evaluate $E(k_{||})$ diagrams from angle-resolved IPE spectra taken with the angle resolution of the used sample manipulator (smallest steps of 2.5°) and the angle divergence of the used electron gun ($0.8 - 1.0 \text{ nm}^{-1}$). At the normal incidence spectrum (see Fig. 12) the five peaks (a)–(e) at energetic positions of (1.0 ± 0.1) , (2.4 ± 0.1) , (3.6 ± 0.1) , (4.8 ± 0.1) , and at (7.4 ± 0.2) eV can be distinguished. The energetic position of the peak (a) is within the bulk bandgap similar to the lowest unoccupied surface band at the other reconstructions. Therefore it can be identified tentatively as surface peaks. The nature of the higher peaks (b) and (d)—surface or bulk—is open at present.

IV. CONCLUSIONS

We can determine dispersion relations of the (1×1) -, $(\sqrt{3} \times \sqrt{3})R30^\circ$ -, and (3×3) -reconstructed 6H-SiC(0001) surface by means of angle-resolved inverse photoemission. The stability concerning taking inverse photoemission spectra of these surfaces decreases in the order (1×1) , (3×3) , $(\sqrt{3} \times \sqrt{3})R30^\circ$. All reconstructions can be easily reprepared in a Si flux at controlled temperatures. Normal incidence IPE spectra of all four known reconstructions show four to six peaks. Series of angle-resolved IPE spectra taken at three surfaces allow a determination of the energy

dispersion of the bands within the first Brillouin zone. We compare the experimental results with calculated single-electron surface band structures (LDA calculations) and a Mott-Hubbard model which takes intra-atomic Coulomb interaction into account. There are a few agreements between single electron LDA calculations for the (1×1) - and $(\sqrt{3} \times \sqrt{3})R30^\circ$ -reconstructed 6H-SiC(0001) surface and the experimentally determined surface band structures, but the LDA calculations predict a half filled surface state $D (\Sigma_1)$ for the $(\sqrt{3} \times \sqrt{3})R30^\circ$ reconstruction, while all experiments show fully occupied and fully empty surface states at this reconstruction. Because the Fermi level of the investigated p -doped sample and the Fermi level determined at a n -doped

sample are nearly the same, a Mott-Hubbard picture fits better the experimental data. The Hubbard parameter can be estimated from experimental data to $U=2.05$ eV [1.25 eV] for the $(\sqrt{3} \times \sqrt{3})R30^\circ [(3 \times 3)]$ reconstruction of the 6H-SiC(0001) surface, which is in good agreement with theoretical values of $U=2.1$ eV [≈ 1 eV] of Furthmüller *et al.* and $U=1.95$ eV of Rohlfig *et al.* for the $(\sqrt{3} \times \sqrt{3})R30^\circ$ reconstruction and somewhat larger than the $U=1.5$ eV of Anisimov *et al.* and $U=1.6$ eV of Northrup *et al.*

ACKNOWLEDGMENTS

We thank M. Rohlfig for fruitful discussions.

¹P. W. Erdman and E. C. Zipf, Rev. Sci. Instrum. **53**, 225 (1982).

²D. Funnemann and H. Merz, J. Phys. E **19**, 554 (1986).

³I. Schäfer, Ph.D. thesis, University of Kiel, Germany, 1986.

⁴Cree Research, Inc. 1996.

⁵J. Pelletier, D. Gervais, and C. Pomot, J. Appl. Phys. **55**, 994 (1984).

⁶V. van Elsbergen, T. U. Kampen, and W. Mönch, Surf. Sci. **365**, 443 (1996).

⁷R. Kaplan, Surf. Sci. **215**, 111 (1989).

⁸M. Sabisch, P. Krüger, and J. Pollmann, Phys. Rev. B **55**, 10 561 (1997); J. Pollmann, P. Krüger, and M. Sabisch, Phys. Status Solidi B **202**, 421 (1997).

⁹J.-M. Themlin, I. Forbeaux, V. Langlais, H. Belkhir, and J.-M. Debever, Europhys. Lett. **39**, 61 (1997); I. Forbeaux, J.-M. Themlin, V. Langlais, L. M. Yu, H. Belkhir, and J.-M. Debever,

Surf. Rev. Lett. **5**, 193 (1998).

¹⁰J. E. Northrup and J. Neugebauer, Phys. Rev. B **52**, R17 001 (1995).

¹¹J. E. Northrup and J. Neugebauer, Phys. Rev. B **57**, R4230 (1998).

¹²M. Rohlfig and J. Pollmann, Phys. Rev. Lett. **84**, 135 (2000).

¹³J. Furthmüller, F. Bechstedt, H. Hüsken, B. Schröter, and W. Richter, Phys. Rev. B **58**, 13 712 (1998).

¹⁴V. I. Anisimov, A. E. Bedin, M. A. Korotin, G. Santoro, S. Scandolo, and E. Tosatti, Phys. Rev. B **61**, 1752 (2000).

¹⁵P. Mårtensson, F. Owman, and L. I. Johansson, Phys. Status Solidi B **202**, 501 (1997); L. I. Johansson, F. Owman, and P. Mårtensson, Surf. Sci. **360**, L478 (1996).

¹⁶L. S. O. Johansson, L. Duda, M. Laurenzis, M. Krieffewirth, and B. Reihl, Surf. Sci. **445**, 109 (2000).